Effects of systematic phase errors on phase-only correlation

Robert W. Cohn and Joseph L. Horner

The performance of phase-only optical correlators is usually reduced if the filter-plane phase differs from that prescribed for the classical matched filter. Current spatial light modulators, which frequently produce less than 2π phase modulation, and interface circuits, which quantize or incorrectly amplify signals placed on the spatial light modulator, both can produce systematic phase errors. We examine these effects using a model of correlation-peak amplitude as a function of phase error. The correlation peak is reasonably approximated as the product of an average of unity-amplitude error phasors multiplied by the average amplitude across the filter plane. The trends predicted by this new model compare favorably with computer simulations that use gray-scale images.

Key words: Phase-only correlators, pattern recognition, spatial light modulators, correlation metrics, coherent optical processors, real-time correlators, binary optics, optimal filters.

Introduction

Limitations of Spatial Light Modulators Used for the Filter Plane

The phase-only correlator consists of an amplitude-only spatial light modulator (SLM) in the input plane and a phase-only transparency in the filter plane.[1] The phase of the filter is, by definition, the negative of the phase spectrum of the object to be recognized. The enthusiasm for the phase-only correlator has centered in great part around its higher diffraction efficiency, its narrower correlation peaks in relation to those for matched-filter correlators, and its ease of writing on available SLM's. However, it has been difficult to realize SLM's that are continuously variable over a 2π range of phase modulation and that cause no residual modulation of amplitude.[2,3] The recognition of these practical limitations is probably a major reason for the current popularity of the binary phase-only filter in optical correlators. Also, in recognition of the problem of limited modulation range of SLM's, several studies have been devoted to developing filter design procedures that maximize various performance metrics under the constraint of limited modulation range.[2–8] The emphasis of the optimal filter design studies is more on minimizing the effects of limited modulation range than on evaluating and understanding the effects on performance. Most similar among these studies in relation to the current study is that of Farn and Goodman,[6] especially in their developing a lower performance bound for correlation with quantized phase-only filters that are optimized by adjustments of a phase offset with respect to the threshold line angle.[5,8] We note below an interesting correspondence between one of Farn and Goodman's results and our's.

Instead, we choose to focus directly on describing the effects of limited-phase modulation characteristics on correlation. We view limited-phase SLM's as producing a phase error $\delta\phi$, which is the difference between ϕ_d, the phase required for (ideally, the 2π range) phase-only correlation and ϕ_a, the phase actually achievable with a constrained SLM. The comparisons presented here make no special provisions for optimizing filter performance in the presence of a limited-phase constraint, especially since our most basic model does not use detailed information about the object to be recognized. However, a more general model is discussed that shows how the spectral distribution of the object with respect to the threshold line angle influences correlator performance.

In general, phase errors arise from unintended transformations of signals to be placed on the SLM. Thus phase errors can also result from the nonideal performance of electronic and optical components

R. W. Cohn is with the Department of Electrical Engineering, University of Louisville, Louisville, Kentucky 40292; J. L. Horner is with Rome Laboratory, Hanscom Air Force Base, Massachusetts 01731-5000.

Received 30 July 1993; revised manuscript received 23 February 1994.

0003-6935/94/235432-08$06.00/0.

between the signal source and the SLM. Therefore this study is applicable to many practical issues that must be considered in the design and the development of actual phase-only correlators. Some possible sources of phase error are suggested in the next subsection, but in general the practical issues relate to calibration of signal levels and to the tolerances and the accuracy of components that process the signal that is ultimately transformed into the phase modulation.

In this paper we are interested specifically in systematic as opposed to random errors. By systematic phase error we mean that the phase-error distribution $\delta\phi(f)$ across the filter plane (of frequency coordinate f) is nonrandom or deterministic. Recent studies on effects of systematic phase errors have focused primarily on simulation and experimental measurement[9,10] rather than on developing models of correlator performance, as is done in this study. The study by Downie *et al.*[6] included the effects of a static pattern of phase errors across the SLM, whereas the study by Horner and Gianino[9] considered cases in which phase error at each pixel is describable as an explicit function of the phase desired. While both static and filter-dependent phase errors are types of systematic error, our study considers specifically the filter-dependent case.

Our proposed model follows from observations that the correlation peaks can be viewed as a summation of a large number of coherent wave fronts. This summation is similar in form to an expected value or an ensemble average. This correspondence with statistical models provides insight into correlation and is used in the development of a simple analytic model of correlator performance. The expressions that describe performance of phase-only correlators as a function of systematic phase-error characteristics are derived below and are shown to have good correspondence with computer simulations.

Phase-Error Characteristics of Interest

Figure 1 illustrates a variety of systematic errors that can be reasonably anticipated in nonideal phase-only SLM's and practical optoelectronic correlation systems. Figure 1(a) shows two types of continuous phase errors. Both curves are typical of SLM's that produce phases only between $\pm k\pi$. The solid curve represents an SLM that matches exactly the signal phase within these limits. The dashed curve has a slope of value k, and thus phase error $\delta\phi$ is proportional to $1 - k$. The solid transfer characteristic could result from either the limited modulation range of the SLM or the saturation of amplifiers in the signal interface circuits. The dashed curve could result from an incorrect amplifier gain setting, and, as drawn, the saturated SLM could also produce the nonunity slope characteristic if its signals were attenuated by the factor k.

Figure 1(b) shows a discontinuous phase transfer curve. This is a generalized characteristic for the binary phase-only filter, in which the two phases may

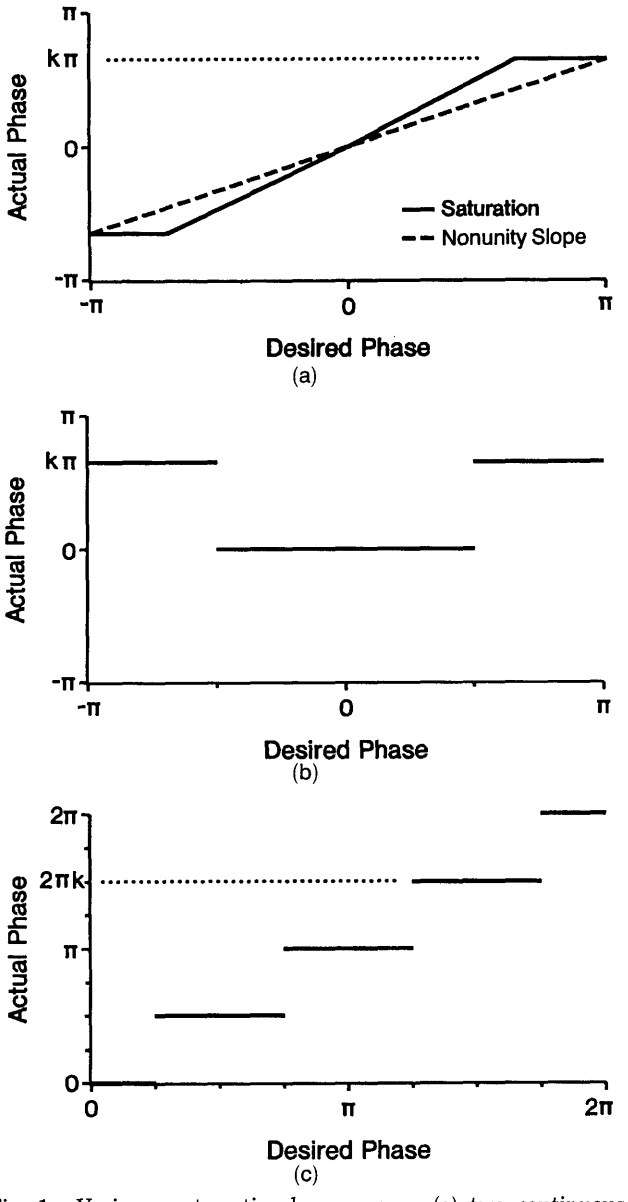

Fig. 1. Various systematic phase errors: (a) two continuous mappings for which the actual phase has less than a 2π range of modulation, (b) binary phase-only mapping in which the range of phase modulation is not necessarily π, (c) mapping in which the actual phase is quantized into m levels [in which Eq. (1) gives the relationship between k and m].

be separated by other than π. Such an error can result from incorrect fabrication of a binary optic or, once again, from incorrect gain of the signal applied to the SLM. Another type of discontinuous phase characteristic is that resulting from quantization of the phase, as illustrated in Fig. 1(c). Quantization is to be expected for filters fabricated by binary optical techniques or for SLM's that are addressed by digital circuits. For this case, k is related to the number of quantization levels, m, as

$$k = \frac{m - 1}{m}. \tag{1}$$

For example, Fig. 1(c) shows four phase levels, and thus k equals 0.75. This relationship is used [specifically, in Eq. (12)] to map the performance curves for quantization errors onto the performance curves for slope errors. In all subsequent analyses, k is always assumed to be less than or equal to one.

A secondary objective of this paper is to compare specifically the effects on performance of the two continuous phase-modulation characteristics shown in Fig. 1(a). It was our trying to understand these differences that first suggested the analysis presented in this paper. We present this comparison as a detailed demonstration and confirmation of our theory. As further background on this problem, we now review what is already known about the effect of these SLM phase errors and how the current design-oriented methodologies could also be used to understand their effects.

Juday has shown that, if the filter-plane SLM produces less than a 2π range of modulation, then the optimal performance under this constraint is obtained by mapping of the optimal phase under no constraints [or in Fig. 1(a), the desired phase] to the achievable (or actual) phase according to the saturated curve.[4] Furthermore, there is a value of phase offset (adjusted with respect to the threshold line angle[5,8]) that minimizes the mean-squared error (or, in Juday's terminology, the Euclidean distance) between the optimal filter and the filters achievable with the SLM. With Juday's approach, after a filter is designed to optimize a specific performance metric, the metric for the optimal achievable filter can be directly calculated and compared with all other filters (achievable or otherwise). However, the value of the metric depends strongly on the exact image to be recognized in each design; thus a new simulation is required for each new image. Juday's approach can be generalized directly to incorporate systematic phase errors. One can do this by altering systematically the phase-modulation curve by the known error and then by redesigning the filter. This approach is perfect for design optimization but becomes cumbersome, requiring numerous simulations, for systems analysis of the dependence of correlation on disparate imagery and SLM phase errors. For this reason we instead choose to develop a simple model that, while sacrificing the numerical accuracy of available approaches, provides general insight into correlator performance. Also, note a difference in comparing our results to the earlier research on optimized phase-only filters[2–8]: In our derivation we make simplifying assumptions about the image spectrum that permit the dependence on threshold line angle to be removed altogether.

Model of Peak-Correlation Amplitude

The performance of optical correlators is characterized by any one of several metrics.[11,12] These usually depend strongly, and for several metrics, exclusively, on the peak amplitude of the correlation surface. Our analyses can then be understood by recognition of the similarity between the peak-correlation amplitude and a specific type of average across the filter plane.

In the phase-only correlator the signal $s(x)$ is Fourier transformed to produce

$$S(f) = a(f)\exp[j\phi(f)] = \mathcal{F}\{s(x)\}, \tag{2}$$

where $a(f)$ is the positive-valued spectral amplitude and $\phi(f)$ is the spectral phase. The phase-only correlator, similar to the matched-filter correlator, is designed so that the filter exactly cancels all phases. This produces a peak-correlation plane amplitude on the optical axis of

$$c(0) = \int_{-B_f/2}^{B_f/2} a(f)\mathrm{d}f = B_f\bar{a} \tag{3}$$

for an SLM of finite extent or spatial bandwidth B_f. The overbar in Eq. (3) is used to indicate the spatial average (across the frequency plane) of the variable a, where the spatial average for a general function $g(f)$ and for a given bandwidth B is defined as

$$\bar{g} \equiv \frac{1}{B}\int_{-B/2}^{B/2} g(f)\mathrm{d}f. \tag{4}$$

This form is identical to the temporal average.[13,14] If the SLM exhibits systematic phase errors, then the peak-correlation amplitude becomes

$$\begin{aligned} c(0) &= \int_{-B_f/2}^{B_f/2} a(f)\exp\{j\delta\phi[\phi(f); \mathrm{k}]\}\mathrm{d}f \\ &= B_f\overline{a\exp(j\delta\phi)}, \end{aligned} \tag{5}$$

where phase error $\delta\phi$ is a function of ϕ and depends on parameter k. For instance, the simplest expression for this is $\delta\phi = (1 - k)\phi$ for the nonunity slope curve [Fig. 1(a)].

A transformation of variables also permits Eq. (5) to be written as

$$\begin{aligned} c(0) &= B_f\int_0^{\infty}\int_{-\pi}^{\pi} a\exp(j\delta\phi)p(\phi, a)\mathrm{d}\phi\mathrm{d}a \\ &= B_f\langle a\exp(j\delta\phi)\rangle. \end{aligned} \tag{6}$$

Thus the spatial average in Eq. (5) is equivalent to the integral in Eq. (6), which takes the form of an ensemble average or an expected value, defined by

$$\langle g\rangle \equiv \int_{-\infty}^{\infty} gp(g)\mathrm{d}g, \tag{7}$$

where $p(g)$ is the probability-density function of the random variable g. Even though a and ϕ are known quantities and are not thought of as random variables, the collection of these variables across the

frequency plane permits them to be mathematically evaluated in the same way as random variables. This correspondence provides useful insights into our modeling method. Thus $p(a, \phi)$ is the joint density of occurrences of the pair of values a and ϕ. A histogram of the ordered pairs (a, ϕ) approximates the joint-density function.

For our purposes of developing a general understanding of how systematic phase errors affect correlation we make the following simplifying approximations to Eq. (6):

$$c(0) \approx B_f \bar{a}\, \overline{\exp(j\delta\phi)} \approx \frac{B_f \bar{a}}{2\pi} \int_{-\pi}^{\pi} \exp(j\delta\phi)\mathrm{d}\phi. \quad (8)$$

A heuristic explanation for the first approximation is that phase influences correlation more strongly than amplitude. This approximation is generally better if the values of phase error do not depend on the values of amplitude. The second approximation is true if the phase ϕ is uniformly distributed over 2π. This assumption is definitely false for reference objects that are real valued, symmetric, and centered on the optical axis. In this case, phase takes on values of 0 and π only. We made histograms of images from commonly available digital-image libraries and found that many do have phases that are rougly uniform in their distribution.

In general, phase does depend on amplitude, and the correspondence between Eq. (5) and approximation (8) is most clearly seen by rewriting of Eq. (6) as

$$c(0) = B_f \int_0^{\infty} a p(a)\mathrm{d}a \int_{-\pi}^{\pi} \exp(j\delta\phi) p(\phi|a)\mathrm{d}\phi, \quad (9)$$

where the standard identity from statistics $p(a, \phi) = p(\phi|a)p(a)$ is used and $p(\phi|a)$ is the density of ϕ conditioned on the value of the parameter a. For cases in which $p(\phi|a)$ does not depend on a, then a and ϕ are by definition independent, in which case the first approximation in approximation (8) is equivalent to Eq. (9). It also not necessary that a and ϕ be independent. It is sufficient that the arguments of the ensemble average are uncorrelated; i.e., $\langle a \exp(j\delta\phi)\rangle = \langle a\rangle \langle \exp(j\delta\phi)\rangle$. Equation (9) can thus be used to resolve differences between our conceptual models based on approximation (8) and experimental results obtained by images with known joint distributions of amplitude and phase. An example in which the form of the joint distribution is an issue is that of designing binary phase-only and ternary filters. It is exactly the distribution of amplitude and phase that determines the optimal choice of phase offset with respect to the threshold line angle.

Correlation-Peak Amplitude as a Function of the Systematic Phase Errors

The expressions for peak-correlation amplitude found by evaluation of approximation (8) with the specific functions of ϕ given in Fig. 1 are

$$c_s(0) = B_f \bar{a}[k + (1 - k)\mathrm{sinc}(1 - k)], \quad (10)$$

$$c_n(0) = B_f \bar{a}\, \mathrm{sinc}(1 - k), \quad (11)$$

$$c_q(0) = B_f \bar{a}\, \mathrm{sinc}\left(\frac{1}{m}\right) = c_n(0)|_{k=m-1/m}, \quad (12)$$

$$|c_b(0)| = \frac{B_f \bar{a}}{\pi/2} \cos\left[\frac{\pi}{2}(1 - k)\right] = \cos\left[\frac{\pi}{2}(1 - k)\right] c_q(0)|_{m=2}, \quad (13)$$

where the correlation amplitude for the saturated characteristic is c_s, the nonunity slope is c_n, the binary phase is c_b, and the quantized case is c_q. As indicated by the second equality in Eq. (12), which uses the definition from Eq. (1), the correlation performance as a function of k is identical for both the nonunity slope characteristic and the quantized characteristic. It is interesting to note that we have derived the same result as Eq. (12) by assuming that phase-mismatch errors from quantization are uniformly distributed random variables of spread $\pm m/2$.[15] In Eq. (13), absolute value signs are included to eliminate a phase-offset term that is not of interest. For k equal to unity the correlation amplitude for the binary characteristic is identical to the two-level quantized characteristic, as expected. Equation (13) shows that the binary phase-only correlator is fairly insensitive to phase offsets that are not exactly π. Also, the amplitude of the binary phase-only correlator (for $k = 1$) is identical to the nonunity slope correlator when $k = 0.5$.

Another systematic error of recent interest is the quadratic phase error that can arise as a result of the quadratic relationship between address voltage of a deformable-mirror pixel and the phase modulation it produces.[9] Approximation (8) can be applied in the same manner as before. The resulting expression contains several Fresnel integrals.

An additional observation is in order on the functional form of Eq. (12). This term appears in previous studies on quantized phase-only filters[6] and kinoforms.[16,17] Of special interest is Farn and Goodman's results on the lower bound of performance for correlators using quantized phase-only filters [their Eq. (39)]. This ratio of signal-to-noise ratio when phase is quantized to signal-to-noise ratio when there is no quantization is identical to the ratio of $c(0)$ in Eq. (12) to $c(0)$ when there is no quantization. It is interesting to note that Farn and Goodman's performance bound is applicable to filters that are optimized under the constraint of quantized phase (i.e., on the basis of the threshold line angle), while under our set of assumptions of uniformly distributed phase and independent amplitude, optimization is not required and does not improve the performance of our model. Therefore our equality for nonoptimized quantized filters coincides with Farn and Goodman's lower bound. Perhaps this result can be used in the

establishment of performance bounds with other types of phase constraint.

Models of Correlation Metrics: Continuous and Discrete Signals

As mentioned above, the effect of systematic phase errors acts only through the peak ampltide for many of the recently discussed correlation metrics.[11,12] We show the dependence on peak amplitude for one of these metrics and also make clear the correspondence between our continuous-signal model and the discrete-signal models that are typically used to simulate optical correlator performance.

Peak-to-noise ratio (PNR) is

$$\mathrm{PNR} = \frac{|c(0)|}{\left\{\frac{1}{B_x - \Delta_x}\left[\int_{-B_x/2}^{B_x/2} |c(x)|^2 \mathrm{d}x - \int_{-\Delta_x/2}^{\Delta_x/2} |c(x)|^2 \mathrm{d}x\right]\right\}^{1/2}}, \tag{14}$$

where the denominator represents the rms amplitude across a correlation plane of spatial bandwidth B_x that excludes a small region of width Δ_x. This metric is the continuous-signal equivalent to peak-to-correlation energy (PCE″) for discrete signals:

$$\mathrm{PCE}'' = \frac{(N-1)^{1/2}\,|c_0|}{\left(\sum_i |c_i|^2 - |c_0|^2\right)^{1/2}}, \tag{15}$$

where $N = B_x/\Delta_x$ is the number of sample points in an image.[11] (The metric PCE″, some of its properties, and its relationship to Kumar and Hassebrook's PCE[12] is described in Ref. 11.) The equivalence between PNR and PCE″ follows by insertion of the standard piecewise approximation for integrals into Eq. (14):

$$g_i \equiv \frac{1}{\Delta_x}\int_{-\Delta_x/2}^{\Delta_x/2} g(x + i\Delta_x)\mathrm{d}x \approx g(i\Delta_x), \tag{16}$$

which is valid as long as the function varies slowly enough over the limits of integration Δ_x. In the case of digital simulations of optical correlation (including those simulations presented here), which typically use the fast-Fourier transform (FFT), B_x represents the extent of the FFT window and Δ_x represents the separation between FFT sample points. For these analyses we also assume that the SLM in the frequency plane has N pixels of pitch Δ_f that extends over a bandwidth B_f. The signal $s(x)$ is also spatially limited to $B_x/2$ or, equivalently, s_i is limited to $N/2$ samples so that the SLM can sample the signal spectrum $S(f)$ at or below the half-Nyquist rate. For these sets of assumptions, PNR is approximately equal to PCE″ to within the limits set by the Nyquist sampling theorem.[18]

For these assumptions, the PNR in Eq. (14) can be rewritten as

$$\mathrm{PNR} = \frac{(N-1)^{1/2}|c(0)|}{[E_c - |c(0)|^2]^{1/2}}, \tag{17}$$

where, through applying Parseval's relation to the phase-only correlator, we can express the correlation energy E_c as

$$E_c = \int_{-B_x/2}^{B_x/2} |c(x)|^2 \mathrm{d}x = \int_{-B_f/2}^{B_f/2} |a(f)\exp(j\delta\phi)|^2 \mathrm{d}f = \int_{-B_f/2}^{B_f/2} a^2(f)\mathrm{d}f. \tag{18}$$

Thus, with reference to Eq. (5), it can now be seen that the dependence of PNR on $\delta\phi$, or, equivalently, the parameter k, is caused by the peak amplitude $c(0)$ only. Explicitly, substituting identity (4), approximation (8), and Eq. (18) into Eq. (17), our model for PNR becomes

$$\mathrm{PNR} \approx \frac{(N-1)^{1/2}|\bar{a}\,\overline{\exp(j\delta\phi)}|}{[\overline{a^2} - |\bar{a}\,\overline{\exp(j\delta\phi)}|^2]^{1/2}}, \tag{19}$$

where the approximate equality is due to approximation (8). Except for this approximation, which we are evaluating in this paper, approximation (19) is equivalent to Eq. (15). For modeling purposes it is most convenient to view the averaging operator as a continuous integral, while for simulation with signals represented by their spectra the averages are well approximated as

$$\bar{g} \approx \frac{1}{N}\sum_{i=1}^{N} g_i, \tag{20}$$

which follows directly from the validity of approximation (16).

Discussion on the Form of Peak-to-Noise Ratio

Our model for PNR, approximation (19), depends on only three parameters: N, the number of pixels in the frequency-plane SLM; k, the parameter that controls the amount of phase error for a given type of systematic error characteristic; parameter

$$Z = \frac{\overline{a^2}}{\bar{a}^2}, \tag{21}$$

which depends solely on the distribution of the values of the spectra. Using our statistical interpretation (correspondence between the spatial average and the ensemble average), we can see that the numerator of Z is simply a variance. Minimizing the standard deviation of the spectral values minimizes Z.

In its most compact form, approximation (19) is then written as

$$\mathrm{PNR}^2 = \frac{(N-1)|\overline{\exp(j\delta\phi)}|^2}{Z - |\exp(j\delta\phi)|^2}. \tag{22}$$

Thus in the phase-only correlator the value of PNR is also influenced by the spectral distribution of the signal that is to be recognized. A white spectrum (over the full width of the phase-only SLM) will produce the smallest value of Z, which is unity, and consequently gives the largest values of PNR. In the case of no phase errors, PNR is infinite, indicating that all energy is focused to a single pixel in the correlation plane and no energy coincides with the other pixels. Infinite PNR is not physically possible if the frequency-plane illumination is of finite extent, but it is nonetheless obtained in simulations as a result of designing our model to match the discrete model used for FFT-based simulations. The infinite value of PNR is a direct result of the discrete Fourier transform of the white spectrum producing the (discrete-signal) delta function.[11]

An example showing the sensitivity of PNR to spectral distribution for a reasonably broad set of model spectra is presented. Since we usually observe low-pass spectra when working with real-world images, we choose a variable-exponent power law:

$$a(f) = \left(1 - \left|\frac{f}{w}\right|^p\right)\mathrm{rect}\left(\frac{f}{2w}\right), \tag{23}$$

where $2w$ represents the spectral width of the signal and p is assumed to be greater than zero. The resulting value of the bandwidth parameter Z is

$$Z = \frac{p+1}{2p+1}\frac{B_f}{w}. \tag{24}$$

The term $(p+1)/(2p+1)$ only varies between 0.5 and 1 for all values of p between 0 and ∞.

This analysis can be extended directly to two-dimensional rectangularly separable spectra with the result that

$$Z = Z_{f_x} Z_{f_y}, \tag{25}$$

where Eq. (24) is specified independently for the f_x and f_y coordinates. For two-dimensional circularly symmetric spectra with radial power-law dependence identical to Eq. (23),

$$Z = \frac{p+2}{p+1}\frac{B_f^2}{\pi w^2}. \tag{26}$$

For $p = \infty$ (the spectrum is essentially a circ function) and $2w = B_f$, Z in Eq. (26) is $4/\pi$. The minimum value of Z is greater than unity for the circular spectrum, but this is to be expected since it has a smaller total bandwidth than the rectangular spectra. Basically, Eqs. (24)–(26) indicate that there is an effective bandwidth for every spectral distribution that produces identical correlator performance. For understanding PNR, the equating of Z values from different distributions determines the definition of effective bandwidth.

Comparison of Modeled and Simulated Peak-to-Noise Ratio

In the simulations the phase-only filters are either the conjugate-phase spectra of the image to be recognized (for $k = 1$) or the conjugate phase with the systematic phase errors, as indicated by Fig. 1(a). In none of the simulations did we add phase offsets to the filter (in order to optimize performance; see discussions above on threshold line angle). The images consist of a 64×64 array of pixels padded by zeros in a 128×128 array. We performed the correlation by fast-Fourier transforming the image and multiplying its spectrum by a 128×128 array of unit-magnitude complex-valued numbers that represent the $N = 16{,}384$ pixels of the phase-only SLM.

Figure 2 shows phase-only correlator performance for the saturated and nonunity slope phase-error characteristics for the specific input image of a woman's face.[19] The curves represent Eq. (21) for the two types of phase errors. We used a value of $Z = 6.23$ in the model in order to produce the same value of PNR as was simulated for no phase errors (i.e., for $k = 1$). This is not a free parameter but rather a recognition that for no phase error, approximation (8) (our principal approximation) is equivalent to Eqs. (3) and (5). We find that the curves for this and other images track favorably the simulated results for the purposes of making relative comparisons between the effects of various systematic phase errors. The fact that the simulated PNR exceeds the modeled PNR is an indication that more of the image spectrum can be phase matched by the limited-phase SLM than for a uniformly distributed spectrum, for this particular image. Other images (or phase offsets) can produce a simulated PNR that is less than the modeled PNR. The finer resolution of these effects, along the lines of

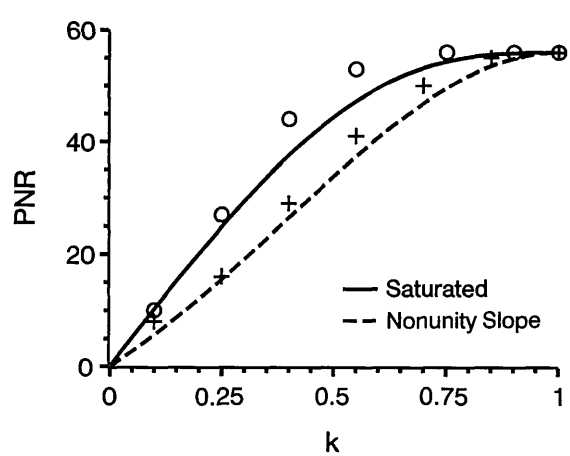

Fig. 2. Comparisons of PNR model (curves) with PNR simulation (data points) for the systematic errors described in Fig. 1(a). The image used for the input and the filter is the face of a woman.[19]

Eq. (9), is probably of practical interest only in sophisticated pattern-recognition problems for which the image data sets have rather specialized properties.

We also observed the same trends, in fact, with even closer agreement, for the phase-only correlation of a tank image[19] with the same tank on a natural cluttered background (Fig. 3). In this case we know that the undesired signal produces additional phase errors and alters the spectral distribution of amplitude. The value of Z is again set to force the model and simulation to be equivalent if there are no systematic phase errors. However, in this case, Z incorporates these additional affects as well. For clutter modeled as a noise process the additional phase errors can be analyzed by the approaches described in Refs. 7 and 20. The closer agreement between the model and the simulation in this case is probably because of the additional randomization of phase that is caused by the addition of clutter.

The simulation with the image of the woman (and images of smaller bandwidth) show that the PNR depends essentially on peak amplitude $c(0)$. For its specific value of $Z = 6.23$, ignoring variations in the denominator of approximation (19) changes the values of the PNR curve only by $\sim 8\%$.

Since spectral bandwidth is used widely, we consider briefly the range of bandwidths for which the denominator of approximation (19) has as small an effect on PNR as does the test image. We do this by determining the relative bandwidth $2w/B_f$ for each spectrum that gives a value of Z equivalent to that of the test image. For brick-wall spectra (i.e., power $p = \infty$) the one-dimensional model has a relative bandwidth of 16%, the square-separable model [Eqs. (24) and (25)] has a relative bandwidth of 40%, and the circular model [Eq. (26)] has a relative bandwidth of 44%. For spectra that are most heavily weighted toward dc (i.e., $p = 0$) the relative bandwidth becomes

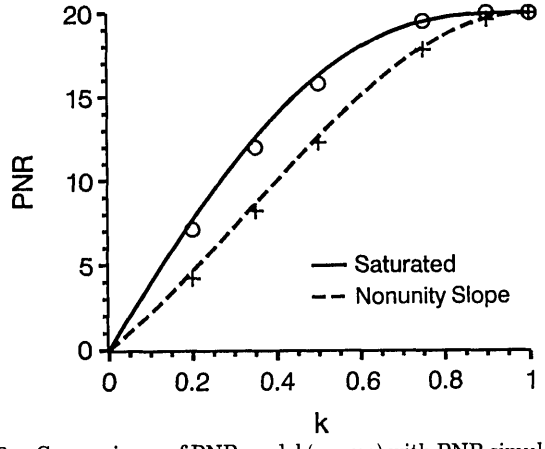

Fig. 3. Comparisons of PNR model (curves) with PNR simulation (data points) for the systematic errors described in Fig. 1(a). The image used for the filter is a tank. The image used for the input is the same tank with clutter added.[19] The model does not include the effect of the clutter. However, for purposes of comparison the value of the model at the end point ($k = 1$) is set equal to that for the simulation.

32% for one-dimensional, 80% for square-separable, and 64% for circular spectra. While the bandwidths vary for the brick-wall-model spectra between 16% and 44%, the effective bandwidth area (for example, the rectangular case $B = B_x B_y = 16\%$), or equivalently, the effective number of SLM pixels illuminated is constant (2621 for a 16,384-pixel SLM).

In summary of this section, we examined the effects on correlation when the filter-plane SLM is incapable of modulation over the full 2π range. We performed a detailed comparison of a phase-only filter correlator for which the desired phase is mapped to a limited-phase SLM in two different ways: linear scaling of phase and saturation of phase. For each value of k and for either model or simulation, the saturated phase mapping produced a greater PNR than the linear mapping, as expected according to Juday's theory. Uniquely in contrast to Juday's approach is that a simple model (requiring only the vaguest of information about the image) was used to quantify the difference in performance for the two different phase characteristics.

Conclusions

These findings indicate that several correlation metrics of interest can be modeled with reasonable accuracy by use of approximation (8). The model reduces to easily computed functions for phase errors of current interest that can arise from limitations in current SLM's and trade-offs between cost and performance of electronic interface circuits. Since the model requires only general knowledge of image properties (namely, the bandwidth parameter Z, which is identical for any number of different images), it relieves system designers from the necessity of performing image-based simulations every time a design parameter, a component specification, or a tolerance changes.

This is not the first evidence that correlation metrics for a variety of images show the same trends. Even though phase errors were not considered, Kumar and Hassebrook found similar trends for simulations of various correlation metrics with a variety of images.[12] It appears that their results can also be explained in terms of an effective image bandwidth. The most interesting and surprising result of this study as observed by Kumar and Hassebrook and ourselves is the very limited dependence of correlation performance on the detailed parameters defining an image. Such results are analogous to nonparametric statistics[21] in which the resulting statistic (the correlation metric) is, at best, only weakly dependent of the functional form of the underlying distribution (the image).

We thank R. D. Juday for helpful technical discussions on generalized optimality criteria for constrained correlation filters, physical insights into correlation metrics, and some clarifying examples of both. R. W. Cohn acknowledges the sponsorship of the Advanced Research Projects Agency through U.S.

Air Force Rome Laboratory contract F19628-92-K-0021.

References and Notes

1. J. L. Horner and P. D. Gianino, "Phase-only matched filtering," Appl. Opt. **23,** 812–816 (1984).
2. M. W. Farn and J. W. Goodman, "Optimal maximum correlation filter for arbitrarily constrained devices," Appl. Opt. **28,** 3362–3366 (1989).
3. R. D. Juday, "Correlation with a spatial light modulator having phase and amplitude cross coupling," Appl. Opt. **28,** 4865–4869 (1989).
4. R. D. Juday, "Optimum realizable filters and the minimum Euclidean distance principle," Appl. Opt. **32,** 5100–5111 (1993).
5. M. W. Farn and J. W. Goodman, "Optimal binary phase-only matched filters," Appl. Opt. **27,** 4431–4437 (1988).
6. M. W. Farn and J. W. Goodman, "Bounds on the performance of continuous and quantized phase-only matched filters," J. Opt. Soc. Am. A **7,** 66–72 (1990).
7. B. V. K. Vijaya Kumar, "Tutorial survey of composite filter designs for optical correlators," Appl. Opt. **31,** 4773–4801 (1992).
8. B. V. K. Vijaya Kumar and Z. Bahri, "Efficient algorithm for designing a ternary-valued filter yielding maximum signal-to-noise ratio," Appl. Opt. **28,** 1919–1925 (1989).
9. J. L. Horner and P. D. Gianino, "Effects of quadratic phase distortion on correlator performance," Appl. Opt. **31,** 3876–3878 (1992).
10. J. D. Downie, B. P. Hine, and M. B. Reid, "Effects and correction of magneto-optic spatial light modulator phase errors in an optical correlator," Appl. Opt. **31,** 636–643 (1992).
11. J. L. Horner, "Metrics for assessing pattern-recognition performance," Appl. Opt. **31,** 165–166 (1992).
12. B. V. K. Vijaya Kumar and L. G. Hassebrook, "Performance measures for correlation filters," Appl. Opt. **29,** 2997–3006 (1990).
13. A. Yariv, *Optical Electronics,* 4th ed. (Saunders, Philadelphia, Pa., 1991), pp. 3, 356–359.
14. A. Papoulis, *Probability, Random Variables, and Stochastic Processes,* 1st ed. (McGraw-Hill, New York, 1965), pp. 323–332.
15. R. W. Cohn, "Random phase errors and pseudorandom phase modulation of deformable mirror spatial light modulators," in *Optical Information Processing Systems and Architectures IV,* B. Javidi, ed., Proc. Soc. Photo-Opt. Instrum. Eng. **1772,** 360–368 (1992).
16. J. W. Goodman and A. M. Silvestri, "Some effects of Fourier-domain phase quantization," IBM J. Res. Dev. **14,** 478–484 (1969).
17. W. J. Dallas, "Phase-quantization: a compact derivation," Appl. Opt. **10,** 673–676 (1971).
18. A. V. Oppenheim and R. W. Schafer, *Digital Signal Processing* (Prentice-Hall, Englewood Cliffs, N.J., 1975), pp. 26–30.
19. University of Southern California Image Processing Institute Image Data Base. The woman's face is image 5.1.4, and the tank is image 7.1.7.
20. R. W. Cohn and R. J. Nonnenkamp, "Statistical moments of the transmittance of phase-only spatial light modulators," in *Miniature and Micro-Optics: Fabrication,* C. Raychoudhuri and W. B. Veldkamp, eds., Proc. Soc. Photo-Opt. Instrum. Eng. **1751,** 289–297 (1992).
21. W. W. Daniel, *Applied Nonparametric Statistics.* 2nd ed. (PWS Kent, Boston, Mass., 1990), pp. 18–21.